Atmos. Meas. Tech. Discuss., 3, 2275–2316, 2010
www.atmos-meas-tech-discuss.net/3/2275/2010/
doi:10.5194/amtd-3-2275-2010

Atmospheric Measurement Techniques Discussions

An overview of measurement comparisons from the INTEX-B/MILAGRO airborne field campaign

M. M. Kleb[1], G. Chen[1], J. H. Crawford[1], F. M. Flocke[2], and C. C. Brown[1,3]

[1]NASA Langley Research Center, Hampton, Virginia, USA
[2]National Center for Atmospheric Research, Boulder, Colorado, USA
[3]Science Systems and Applications, Inc., Hampton, Virginia, USA

Received: 22 April 2010 – Accepted: 4 May 2010 – Published: 18 May 2010

Correspondence to: M. M. Kleb (mary.m.kleb@nasa.gov)

Published by Copernicus Publications on behalf of the European Geosciences Union.

Abstract

As part of the NASA's INTEX-B mission, the NASA DC-8 and NSF C-130 conducted three wing-tip to wing-tip comparison flights. The intercomparison flights sampled a variety of atmospheric conditions (polluted urban, non-polluted, marine boundary layer, clean and polluted free troposphere). These comparisons form a basis to establish data consistency, but also should also be viewed as a continuation of efforts aiming to better understand and reduce measurement differences as identified in earlier field intercomparison exercises. This paper provides a comprehensive overview of 140 intercomparisons of data collected during INTEX-B. For interpretation and most effective use of these results, the reader is strongly urged to consult with the instrument principle investigator.

1 Introduction

The Intercontinental Chemical Transport Experiment-B (INTEX-B) was the second major airborne field mission conducted in the spring of 2006 as part of the NASA-led INTEX-NA (North America) mission, aiming to investigate the transport and transformation of pollution over the North American continent. INTEX-B operated in coordination with a larger program, the MILAGRO (Mega-city Initiative: Local and Global Research Observations) and IMPEX (Intercontinental and Mega-city Pollution Experiment) missions. INTEX-B was comprised of two phases. Phase one occurred from 1–21 March to maximize overlap with the MILAGRO campaign. During this phase, observations were primarily over Mexico and the Gulf of Mexico. The second phase lasted from 15 April to 15 May and focused on Asian pollution transported across the Pacific Ocean. Five specific goals were identified for INTEX-B: (1) to investigate the extent and persistence of the outflow of pollution from Mexico; (2) to understand the transport and evolution of Asian pollution, the related air quality, and climate implications in western North America; (3) to relate atmospheric composition to chemical sources and sinks; (4) to characterize the effects of aerosols on radiation; and (5) to validate satellite observations of tropospheric composition (Singh et al., 2009). For a complete mission overview, reader is referred to Singh et al. (2009).

The INTEX-B field mission involved two comparably equipped aircraft, the NASA DC-8 and NSF C-130. The sampling strategy often required coordination of both aircraft while making measurements in different regions or times. This naturally led to the pre-planning and execution of a series of comprehensive measurement comparisons of species/parameters measured on both platforms. The overarching goal was to generate a program-wide unified data set from all available resources to better address the science objectives. These comparisons form a basis to establish data consistency. The INTEX-B measurement comparison exercise should also be viewed as a continuation of efforts aiming to better understand and reduce measurement differences as identified in earlier field intercomparison exercises (e.g. NASA TRACE-P, Eisele et al. (2003), and ICARTT, http://www-air.larc.nasa.gov/missions/intexna/meas-comparison.htm). It is recognized that further comparisons of the in-situ data sets to satellite retrievals, lidar, and model output are equally important, however such analyses are beyond the scope of this paper.

2 Background

NASA has a long history of conducting instrument intercomparisons beginning with ground-based intercomparisons in July 1983 (Hoell et al., 1984, 1985a, b; Gregory et al., 1985) prior to the commencement of the airborne field studies in October 1983 with the Chemical Instrumentation Test and Evaluation (CITE) missions (Beck et al., 1987; Hoell et al., 1990, 1993; Gregory et al., 1993a, b, c). These early instrument intercomparisons were conducted on a common aircraft platform and played an important role in understanding the sensitivity of different techniques and evaluating them to find the best possible field instrument. The early intercomparison effort stimulated the development of atmospheric measurement techniques/instruments benefitting airborne field

AMTD
3, 2275–2316, 2010

programs to this day. Since early 2000, integrated field campaigns have made use of the same measurement technique on separate aircraft platforms or different measurement techniques sometimes on the same or separate aircraft platforms. To understand the differences seen in the data and to better utilize the data from various instruments, a careful and thorough intercomparison is needed. The first two-aircraft intercomparison was conducted during the 2001 TRACE-P (Transport and Chemical Evolution over the Pacific) field campaign (Eisele et al., 2003). During TRACE-P the NASA DC-8 and P-3B flew wing-tip to wing-tip within 1 km of each other on three occasions lasting between 30 and 90 min. A significant finding of this exercise was that an intercomparison between two aircraft can reveal important insight into instrument performance. It also verified that two aircraft can be flown in a manner such that both sample the same airmass and experience the same high and low frequency fluctuations necessary to evaluate common measurements. In general the best agreement was achieved for the most abundant species (CO_2 and CH_4) with mixed results for less abundant species and those with shorter lifetimes (Eisele et al., 2003). The TRACE-P comparison of fast (1 s) measurements for CO and O_3 provided valuable information in defining bulk airmass properties, which was useful in interpreting the comparison results for short-lived species. The effect of small scale spatial variation should not have significant impact on assessment of the systematic difference, especially when the range of comparison is sufficiently larger than these variations.

Following TRACE-P, another major coordinated intercomparison occurred in 2004 during the International Consortium for Atmospheric Research on Transport and Transformation (ICARTT) airborne missions (INTEX-A, NEAQS-ITCT 2004, and ITOP). Five wing tip to wing tip intercomparison flights were conducted allowing comparisons between four aircraft. Although not formally published, these intercomparisons and additional mission information can be found in the Measurement Comparisons: ICARTT/INTEX-A link at http://www-air.larc.nasa.gov/missions/intexna/intexna.htm.

The purpose of this paper is to provide a straightforward and comprehensive overview of measurement consistency as characterized through the analysis of the

AMTD
3, 2275–2316, 2010

intercomparison data. This paper is not intended as a review of instrument operation but rather a means to highlight the demonstrated instrument performance during the intercomparison periods. Intercomparison results are intended to identify measurements where an investment in improving measurement capability would be of great benefit. Results are also crucial to ensuring that analysis and modeling activities based on multi-platform observations reach conclusions that can be supported within the assessed data uncertainties. For parties interested in making use of the data presented here, further consultation with the relevant measurement investigators is strongly recommended. The remainder of this paper presents the details of the INTEX-B intercomparison.

Section 3 describes the intercomparison approach and implementation, including a description of the types of comparisons is presented. Data processing procedures and statistical assessment are presented in Sect. 4. Section 5 contains the results, and the summary is contained in Sect. 6.

3 Approach/implementation

During the INTEX-B/MILAGRO/IMPEX field campaigns, three formal measurement comparisons were carried out on 19 March, 17 April, and 15 May 2006. These segments were well integrated into science flights to achieve the overall science goals while aiming to compare instruments/measurements under a wide variety of conditions as summarized in Table 1. During the intercomparison portion of the flights, aircraft separation was less than 300 m in the horizontal and less than 100 m in the vertical. The intercomparison period for the 19 March flight was 41 min (Fig. 1a), covered altitudes from 0.3 to 3.4 km, and encountered Mexico City pollution as well as marine boundary layer air off the coast of Mexico. The wide range of the chemical conditions is evident in CO levels observed during the intercomparison period which ranged from 103 to 223 ppbv. The 17 April (Fig. 1b) intercomparison period lasted 44 min with conditions ranging from polluted at 3.5 km over northern California to clean at 6 km over

Discussion Paper | Discussion Paper | Discussion Paper | Discussion Paper |

AMTD

3, 2275–2316, 2010

Measurement comparisons from INTEX-B/MILAGRO

M. M. Kleb et al.

southern Oregon. Again the range in chemical conditions can be inferred from the CO levels encountered (99 to 163 ppbv). The last intercomparison flight on 15 May (Fig. 1c) was the longest, lasting approximately one hour. This intercomparison began in the clean free troposphere (about 5.5 km) off the northern Oregon coast and ended in the marine boundary layer (near 0.3 km) off the northern California coast. As with the two previous intercomparisons, a variety of chemical conditions existed. For these comparisons, data from all three flights were combined for analysis and only data with values greater than the limit of detection were used for analysis. The comparisons cover short-lived to long-lived gas phase species as well as particulate microphysical, optical, and chemical properties. Table 2 provides a detailed list of the species/parameters included in the intercomparison along with measurement techniques, aircraft platform, principle investigators (PI), and measurement uncertainties. All of the above information was taken from the PI file headers. For an explanation of "Technique", the reader is referred to the individual PI files located on the INTEX-B website (http://www-air.larc.nasa.gov/missions/intex-b/intexb.html) under the Current Archive Status link.

It is imperative that both aircraft sample the same airmass during the intercomparison period. In practice, this is conducted by keeping the aircraft in close proximity while maintaining a safe separation. Analysis of the fastest measurements can be an effective way to ensure the same airmass was sampled by both aircraft. If the same airmass is sampled, we expect the large scale features to be captured by both instruments. This is illustrated in the time series plots for both ozone (19 March) and water (15 May) where the major features are well represented by both instruments in each comparison (Figs. 2a and 3a). While the most prominent features are apparent in the data from each instrument, there is less agreement in the relatively small scale changes that occur when O_3 remains consistently low (at low altitude in the marine boundary layer) and also at higher altitudes and higher O_3 levels (polluted Mexico City airmass). The timeseries for water displays a similar behavior. The large-scale features in the timeseries are well matched while there is less agreement in the finer features

AMTD
3, 2275–2316, 2010

at both high (clean free troposphere) and low altitudes (marine boundary layer). The correlation plots (Figs. 2b and 3b) with associated regressions and coefficients of correlation (R^2) offer an additional method for evaluating the likelihood that the instruments sampled the same airmass. Both ozone and water show that the measurements are strongly correlated as evident by the high R^2 value. Although it is not easy to discern in the time series for water, there is a slight time lag in one of the water measurements. This is evident in Fig. 3b where data points depart the tighter cluster in curved lines. In general the spread in the data appears larger for water than ozone, however, this may be due in part to the smaller range in the x and y scales for water. The high R^2 value for both ozone and water nevertheless indicate that the two aircraft are most likely sampling the same airmass.

Intercomparison analysis was conducted during each stage of data submission: (1) comparison of field data (blind), (2) comparison of preliminary data (not blind), and (3) comparison of final data (not blind). These analyses and the distribution of results were carried out by the Measurement Comparison Working Group (MCWG). The primary responsibility of the MCWG included providing for secure field data submission to facilitate the "blind" comparison, analyzing data for each stage of data submission, and disseminating the results within the science team and to the atmospheric community at large. In stage one, the blind comparison of field data, PIs submitted data within 24 h to a few days after the flight to an ftp site which was "blind" to the science team for a period of time until both paired comparison data were submitted. For example, the CO data was not available to the science team until both NSF C-130 and NASA DC-8 PIs submitted their CO data for the intercomparison flight. The MCWG then assessed the consistency between the paired DC-8 and C-130 measurements/instruments and released the comparison results and the data to the science team. In the preliminary data stage, data were compared again after allowing the PIs to apply post mission calibration and additional processing/correction procedures to their data. The MCWG presented these results to the science team at the post-mission data workshop. In the comparison of final data (not blind), PIs submitted final data with uncertainty estimates. These results are archived online (http://www-air.larc.nasa.gov/missions/intex-b/intexb-meas-comparison.htm) and summarized here.

In addition to the inter-platform comparisons, intra-platform comparisons were made whenever possible. Since both instruments were located on the same aircraft, these comparisons were not limited to the three intercomparison periods discussed previously, rather they could span the entire mission.

As previously stated, the primary goal of this paper is to present a comprehensive overview of the INTEX-B/MILAGRO/IMPEX intercomparison results. The level of the agreement between the measurements may depend on a number of factors, including calibration, instrument time response, and measurement techniques. For the comparison of the aerosol measurements, the particle size range of the measurements should be a critical consideration. In addition, this overview paper does not attempt to describe the complexities of the various measurement techniques. Any interpretation of the results of these studies should be done in consultation with the individual instrument PIs. This information is provided in Table 2.

4 Data process procedures and statistical assessment

The quantitative assessment of measurement/instrument consistency was based on statistical analysis of the intercomparison data. This required the merging of data to a common timeline. Merging was easiest when measurements were conducted with the same timing and integration period; however, it is not unusual for instruments based on different techniques to require different integration times to measure the same species/parameter or that instruments on different platforms are not well synchronized. For cases where instruments had the same integration period, but were not synchronized, the data were merged to ensure at least 50% sampling time overlap. For paired measurements with different integration time intervals, the shorter integration time measurements were merged into the longer time interval when measurements at the shorter time interval overlapped at least 50% of the longer time interval. These merged data pairs were used to quantitatively assess measurement consistency through linear regression analysis, when applicable, or descriptive statistics based on the ratio (DC-8/C-130) of the paired data points. The linear regression slopes and intercepts can be used to describe the level of the measurement agreement when a high enough level of correlation exists. Here, this criteria has been defined as an R^2 value of 0.75. Lower R^2 values are typically encountered when the range of variation is limited in comparison to the uncertainties of the measurements and/or other instrument issues exist. When R^2 is below the threshold of 0.75, the median and percentile values of the DC-8/C-130 ratio have been used to express the level of consistency between the paired data. In addition, the absolute (or arithmetic) difference between paired data may be used in some cases (with combined uncertainties) to gain additional insight.

Statistical comparisons presented here have been based on Orthogonal Distance Regression (ODR). Orthogonal distance regression is a regression technique similar to ordinary least squares (OLS) fit with the stipulation that both x and y are independent variables with errors. ODR minimizes sum of the squares of the orthogonal distances rather than the vertical distances (as in OLS). ODR is generally equivalent to

$$\min_{\beta,\delta,\varepsilon}\frac{1}{2}\sum_{i=1}^{n}\left(w_{\varepsilon_i}\varepsilon_i^2+w_{\delta_i}\delta_i^2\right) \quad (1)$$

subject to $y_i+\varepsilon_i=f(x_i+\delta_i;\beta)$ where ε_i is the error in y, δ_i the error in x, w_{ε_i} and w_{δ_i} weighting factors, and β a vector of parameters to be determined (slope and intercept in this case), (Zwolak et al., 2007). Note that a weighted ODR (w_{ε_i} and $w_{\delta_i}\neq 1$) is necessary when observations x_i and y_i are heteroscedastic (variance changes with i), (Boggs et al., 1988). It has been shown that ODR performs at least as well and in many cases significantly better than Ordinary Least Squares (OLS), especially when $d=\sigma_\varepsilon/\sigma_\delta<2$, (Boggs et al., 1988). Boggs et al. (1988) have shown that ODR results in smaller bias, variance, and mean square error (mse) than OLS, except possibly when significant outliers are present in the data. For the bias of the parameter, β, and function estimates, $f(x_i;\beta)$, OLS is statistically better only 2% of the time while ODR is

AMTD
3, 2275–2316, 2010

significantly better 50% of the time. Results for the variance and mse of the parameter and function estimates were similar; ODR variance and mse were smaller than that from OLS about 25% of the time. OLS results were significantly better than ODR only 2% of the time, (Boggs et al., 1988).

While ODR allows for the possibility of assigning specific uncertainties to each data point, an accurate estimate of measurement uncertainty is not often available on point by point basis. Even when available, this can be complicated when merging measurements of differing integration times. Therefore, in the interest of treating all the intercomparisons uniformly, we use w_{ε_i} and w_{δ_i}=1. The coefficient of determination, R^2, is used to indicate the quality of the linear relationship between the paired measurements.

5 Results

5.1 INTEX-B intercomparison

Three types of comparisons were conducted and are presented below: DC-8 to C-130 (Table 3), DC-8 to DC-8 (Table 4), and C-130 to C-130 (Table 5). One hundred and forty parameters were grouped according to chemical similarities and compared. The chemical groups for intercomparison purposes are photochemical precursors, photochemical products, photochemical radicals, oxygenated volatile organic carbons (OVOCs), non-methane hydrocarbons (NMHCs), photolysis frequencies, particle number and size distribution, particle chemical composition, and particle scattering and absorption.

As stated previously, when R^2 is greater than or equal to 0.75, the slope and intercept of the regression are given to represent the level of measurement consistency. It is noted here that the intercept should not simply interpreted as the offset between the instruments. When R^2 is less than 0.75 percentile statistics are given based on the ratio of the data (DC-8/C-130). The resulting statistics are given in the following Table 3a through i for the DC-8 to C-130 comparison. All analyses are based on the archived

AMTD
3, 2275–2316, 2010

final data combined from all three intercomparison flights. No statistical analyses are provided when there are an insufficient number of data points to adequately represent the entire intercomparison periods. Finally, the range (minimum and maximum) is provided as additional information for the reader. In addition to the comparisons listed in Tables 3, 4, and 5, the uncertainties for each instrument can be found in Table 2. The uncertainties were provided in the final data file archive (Current Archive Status link) online at the INTEX-B website (http://www-air.larc.nasa.gov/missions/intex-b/intexb.html). For cases where uncertainties were available on a point by point basis, the uncertainty was calculated as a percentage of the measurement. The minimum and maximum percentages are given in parentheses and the median is listed outside the parentheses. We present these comparisons and uncertainties without rating the level of agreement. This is a highly subjective task and we leave it to the reader to make that judgment with appropriate consultation with the respective PIs. For an explanation of "Technique", the reader is referred to the individual PI files located on the INTEX-B website (http://www-air.larc.nasa.gov/missions/intex-b/intexb.html) under the Current Archive Status link.

All intercomparison correlation plots can be found online under the Measurement Comparisons: MILAGRO/INTEX-B/IMPEX link at http://www-air.larc.nasa.gov/missions/intex-b/intexb.html. The correlation of the combined the data from all three flights is in the summary section. Individual timeseries and correlation plots are also available for each intercomparison on 19 March, 17 April, and 15 May 2006.

As described earlier, intra-platform comparisons were also conducted on both the DC-8 and C-130 aircraft for any overlapping measurements. See Table 4a through c for a complete list of the species, techniques used, and a statistical summary for the DC-8 to DC-8 comparisons. Table 5a–e provide statistical summary for the C-130 to C-130 comparisons. Since the instruments were located on the same platform, comparison data was not limited to the intercomparison portions of the flights. Data from the entire mission could be included.

AMTD
3, 2275–2316, 2010

5.2 Comparison with ICARTT data

In addition to the intercomparisons made during INTEX-B, we wish to examine the cases where the same comparisons could be made with data from the ICARTT mission and highlight instances where those intercomparisons show significant change. The ICARTT mission was conducted in 2004, a portion of which was INTEX-A (the predecessor to INTEX-B). For a complete description of INTEX-A see Singh et al. (2006). A full listing of the INTEX-A intercomparisons can be found at http://www-air.larc.nasa.gov/missions/intexna/meas-comparison.htm. There are three cases where significant change is observed between INTEX-A and INTEX-B; H_2O_2, PAN, and total PANs. For H_2O_2 the comparison was a DC-8 intraplatform comparison between CIT CIMS and URI EFD during INTEX-A (Fig. 4a) while for INTEX-B, CIT CIMS was on the C-130 and URI EFD on the DC-8 (Fig. 4b). The INTEX-A comparison included significantly more data pairs and covered a wider range of values since both instruments were on the same aircraft and all mission data could be used. During INTEX-B, R^2 is much improved (0.92 in INTEX-B vs. 0.77 during INTEX-A) however the slope of the regression was better during INTEX-A (1.01 for INTEX-A vs. 1.24 for INTEX-B)). This could be due to the smaller amount of data during INTEX-B as well as the smaller dynamic range for the INTEX-B intercomparison measurements.

For PAN, the same instruments were used for both missions ARC PANAK (or dual GC) on the DC-8 for both INTEX-A and INTEX-B; NCAR CIGAR on the NOAA WP-3D for INTEX-A and on the C-130 for INTEX-B). In this case, the INTEX-A intercomparison was better than the INTEX-B intercomparison. During INTEX-B, R^2=0.77 and slope=1.68, while for INTEX-A R^2=0.82 and slope=0.99. During INTEX-B most data was below 500 pptv (19 March flight had values up to about 1400 pptv). For INTEX-A most data was also below 500 pptv with a few points up to about 750 pptv. During INTEX-B the higher values skewed the regression slope. Removing the 5 points where either the DC-8 or C-130 value is above 500 pptv increases R^2 slightly to 0.79 and decreases the slope to 1.23.

AMTD
3, 2275–2316, 2010

The total PANs intercomparisons for INTEX-A and INTEX-B included the same instruments for both missions, with instruments on separate planes for both missions. Both intercomparisons are generally consistent (INTEX-B R^2=0.94, slope=1.35; INTEX-A R^2=0.87, slope=0.95). R^2 was better for INTEX-B while the slope of the regression was better for INTEX-A. The range of values during INTEX-B is almost twice the range during INTEX-A. Again, during INTEX-B a few high values from the 19 March flight skew the slope of the regression. By removing the seven points above 1000 pptv, the slope is reduced to 1.15, (R^2 is also reduced to a value of 0.84).

6 Summary

This paper provides a comprehensive overview of approximately 140 intercomparisons of data acquired during the INTEX-B airborne field campaign conducted in the spring of 2006. A complete set of timeseries and correlation figures can be found at http://www-air.larc.nasa.gov/missions/intex-b/intexb.html under the Measurement Comparisons: MILAGRO/INTEX-B/IMPEX link. For interpretation and most effective use of these results, the reader is strongly urged to consult with the instrument PIs. We leave it to the reader to determine the level of consistency between the instruments compared. This should be done not only with the statistical analyses provided in Tables 3, 4, and 5, but also in consideration of the uncertainties, if available.

AMTD
3, 2275–2316, 2010

Appendix A

Acronyms and abbreviations

Abs 470nm	Aerosol absorption coefficient at 470 nm
Abs 530nm	Aerosol absorption coefficient at 530 nm
Abs 660nm	Aerosol absorption coefficient at 660 nm
ACCD	Aqueous Collection Chemiluminescence Detection
ACD	Atmospheric Chemistry Division
AMS	Aerodyne High-Resolution Aerosol Mass Spectrometer
APS	Aerodynamic Particle Sizer
ARC	Ames Research Center
ARIM	Atmospheric Radiation Investigation and Measurements
ATHOS	Airborne Tropospheric Hydrogen Oxides Sensor
CIGAR	CIMS Instrument by Georgia Tech and NCAR
CIMS	Chemical Ionization Mass Spectrometry
CIT	California Institute of Technology
CITE	Chemical Instrumentation Test and Evaluation
CLD	Chemiluminescence Detector
CN	Condensation Nuclei
CPC	Condensation Particle Counter
Cryo	Cryo-hygrometer
DACOM	Differential Absorption CO Measurement
DFG	Difference Frequency Generation Absorption Spectrometer
DLH	Diode Laser Hygrometer
DMA	Differential Mobility Analyzer
DMS	Dimethyl sulfide
EFD	Enzyme Fluorescence Detection
FT	Free troposphere
GIT	Georgia Institute of Technology
HCN	Hydrogen cyanide
Hot CN	Condensation nuclei with heated inlet to 300 °C
ICARTT	International Consortium for Atmospheric Research on Transport and Transformation
IMPEX	Intercontinental and Mega-city Pollution Experiment

AMTD
3, 2275–2316, 2010

INTEX-A	Intercontinental Chemical and Transport Experiment – A
INTEX-B	Intercontinental Chemical and Transport Experiment – B
INTEX-NA	Intercontinental Chemical and Transport Experiment – North America
ITOP	Intercontinental Transport of Ozone and Precursors
LaRC	Langley Research Center
MC	Mist Chamber
MCWG	Measurement Comparison Working Group
MEK	Methyl ethyl ketone
MILAGRO	Mega-city Initiative: Local and Global Research Observations
MBL	Marine Boundary Layer
N_150C_DMA	Aerosol number density, inlet heated to 150 °C, measured with differential mobility analyzer
N_150C_OPC	Aerosol number density, inlet heated to 150 °C, measured with optical particle counter
N_300C_DMA	Aerosol number density, inlet heated to 300 °C, measured with differential mobility analyzer
N_300C_OPC	Aerosol number density, inlet heated to 300 °C, measured with optical particle counter
N_400C_OPC	Aerosol number density, inlet heated to 400 °C, measured with optical particle counter
N_APS	Aerosol number density, measured with aerodynamic particle sizer
N_DMA	Aerosol number density, measured with differential mobility analyzer
N_OPC	Aerosol number density, measured with optical particle counter
NASA	National Aeronautics and Space Administration
NCAR	National Center for Atmospheric Research
NEAQS – ITCT 2004	New England Air Quality Study – Intercontinental Transport and Chemical Transformation, 2004
NMHCs	Non-methane hydrocarbons
NOAA	National Oceanic and Atmospheric Administration
NO_y	Reactive nitrogen
NSERC	National Suborbital Education and Research Center
NSF	National Science Foundation
Nsub	Submicron aerosol number density
Nsub_150C	Submicron aerosol number density, inlet heated to 150 °C

AMTD
3, 2275–2316, 2010

Measurement comparisons from INTEX-B/MILAGRO

M. M. Kleb et al.

Nsub_300C	Submicron aerosol number density, inlet heated to 300 °C
Nsub_400C	Submicron aerosol number density, inlet heated to 400 °C
Nsuper	Supermicron aerosol number density
Nsuper_150C	Supermicron aerosol number density, inlet heated to 150 °C
Nsuper_300C	Supermicron aerosol number density, inlet heated to 300 °C
Nsuper_400C	Supermicron aerosol number density, inlet heated to 400 °C
ODR	Orthogonal Distance Regression
OLS	Ordinary Least Squares
OPC	Optical Particle Counter
OVOC	Oxygenated Volatile Organic Carbon
PAN	Peroxyacetyl Nitrate
PANAK	PAN/Aldehyde/Ketone Photo Ionization Detector
PILS	Particle-Into-Liquid Sampler
PSAP	Particle Soot Absorption Photometer
PTRMS	Proton Transfer Reaction Mass Spectrometry
RAF	Research Aviation Facility
RR Nephelometer	Radiance Research nephelometer
SAFS	Scanning actinic flux spectroradiometer
Scatt 450nm	Aerosol scattering coefficient at 450 nm
Scatt 550nm	Aerosol scattering coefficient at 550 nm
Scatt 700nm	Aerosol scattering coefficient at 700 nm
Scattsub 550nm	Submicron aerosol scattering coefficient at 550 nm
SSA	Single Scattering Albedo
TD-LIF	Thermal Dissociation-Laser Induced Fluorescence
TDL	Tunable Diode Laser Absorption Spectrometer
TOGA	Trace Organic Gas Analyzer
TRACE-P	Transport and Chemical Evolution over the Pacific
TSI Nephelometer	TSI, Inc. nephelometer
UC	University of California
UCI	University of California, Irvine
UND	University of North Dakota
UNH	University of New Hampshire
URI	University of Rhode Island
USNA	United States Naval Academy

AMTD
3, 2275–2316, 2010

V_APS	Aerosol volume density, measured with aerodynamic particle sizer
V_DMA	Aerosol volume density, measured with differential mobility analyzer
V_OPC	Aerosol volume density, measured with optical particle counter
V_150C_DMA	Aerosol volume density, inlet heated to 150 °C, measured with differential mobility analyzer
V_150C_OPC	Aerosol volume density, inlet heated to 150 °C, measured with optical particle counter
V_300C_DMA	Aerosol volume density, inlet heated to 300 °C, measured with differential mobility analyzer
V_300C_OPC	Aerosol volume density, inlet heated to 300 °C, measured with optical particle counter
V_400C_OPC	Aerosol volume density, inlet heated to 400 °C, measured with optical particle counter
UVF	Ultra-violet fluorescence
Vsub	Submicron aerosol volume density
Vsub_150C	Submicron aerosol volume density, inlet heated to 150 °C
Vsub_300C	Submicron aerosol volume density, inlet heated to 300 °C
Vsub_400C	Submicron aerosol volume density, inlet heated to 400 °C
Vsuper	Supermicron aerosol volume density
Vsuper_150C	Supermicron aerosol volume density, inlet heated to 150 °C
Vsuper_300C	Supermicron aerosol volume density, inlet heated to 300 °C
Vsuper_400C	Supermicron aerosol volume density, inlet heated to 400 °C
WAS	Whole Air Sampling

Acknowledgements. The authors wish to thank the National Aeronautics and Space Administration (NASA) Tropospheric Chemistry (TCP) and Making Earth System data records for Use in Research Environments (MEaSUREs) Programs for their support of the measurements and intercomparisons presented in this paper. We also thank the National Science Foundation Atmospheric Chemistry Program for support of this study. Finally, we would like to thank the pilots and crew of the NASA DC-8 and the NSF C-130 and the INTEX-B and IMPEX/MILAGRO science teams for contributing to the success of this study.

References

Beck, S. M., Bendura, R. J., McDougal, D. S., Hoell, J. M., Gregory, G. L., Curfman, H. J., Davis, D. D., Bradshaw, J., Rodgers, M. O., Wang, C. C., Davis, L. I., Campbell, M. J., Torres, A. L., Carroll, M. A., Ridley, B. A., Sachse, G. W., Hill, G. F., Condon, E. P., and Rasmussen, R. A.: Operational Overview of NASA GTE/CITE 1 Airborne Instrument Intercomparisons: Carbon Monoxide, Nitric Oxide, and Hydroxyl Instrumentation, J. Geophys. Res., 92, 1977–1985, 1987.

Boggs, P. T., Spiegelman, C. H., Donaldson, J. R., and Schnabel, R. B.: A computational examination of orthogonal distance regression, J. Econometrics, 38, 169–201, 1988.

DeCarlo, P. F., Dunlea, E. J., Kimmel, J. R., Aiken, A. C., Sueper, D., Crounse, J., Wennberg, P. O., Emmons, L., Shinozuka, Y., Clarke, A., Zhou, J., Tomlinson, J., Collins, D. R., Knapp, D., Weinheimer, A. J., Montzka, D. D., Campos, T., and Jimenez, J. L.: Fast airborne aerosol size and chemistry measurements above Mexico City and Central Mexico during the MILAGRO campaign, Atmos. Chem. Phys., 8, 4027–4048, doi:10.5194/acp-8-4027-2008, 2008.

Dunlea, E. J., DeCarlo, P. F., Aiken, A. C., Kimmel, J. R., Peltier, R. E., Weber, R. J., Tomlinson, J., Collins, D. R., Shinozuka, Y., McNaughton, C. S., Howell, S. G., Clarke, A. D., Emmons, L. K., Apel, E. C., Pfister, G. G., van Donkelaar, A., Martin, R. V., Millet, D. B., Heald, C. L., and Jimenez, J. L.: Evolution of Asian aerosols during transpacific transport in INTEX-B, Atmos. Chem. Phys., 9, 7257–7287, doi:10.5194/acp-9-7257-2009, 2009.

Eisele, F. L., Mauldin, L., Cantrell, C., Zondlo, M., Apel, E., Fried, A., Walega, J., Shetter, R., Lefer, B., Flocke, F., Weinheimer, A., Avery, M., Vay, S., Sachse, G., Podolske, J., Diskin, G., Barrick, J. D., Singh, H. B. Brune, W., Harder, H., Martinez, M., Bandy, A., Thornton, D., Heikes, B., Kondo, Y., Reimer, D., Sandholm, S., Tan, D., Talbot, R., and Dibb, J.: Summary of measurement intercomparisons during TRACE-P, J. Geophys. Res., 108, 8791, doi:10.1029/2002JD003167, 2003.

Gregory, G. L., Hoell, J. M., Beck, S. M., McDougal, D. S., Meyers, J. A., and Bruton, D. B.: Operational Overview of Wallops Island Instrument Intercomparison: Carbon Monoxide, Nitric Oxide, and Hydroxyl Instrumentation, J. Geophys. Res., 90, 12808–12818, 1985.

Gregory, G. L., Davis, D. D., Beltz, N., Bandy, A. R., Ferek, R. J., Thornton, D. C.: An Intercomparison of Aircraft Instrumentation for Tropospheric Measurements of Sulfur Dioxide, J. Geophys. Res., 98, 23325–23352, 1993a.

Gregory, G. L., Davis, D. D., Thornton, D. C., Johnson, J. E., Bandy, A. R., Saltzman, E. S., Andreae, M. O., and Barrick, J. D.: An Intercomparison of Aircraft Instrumentation for Tropospheric Measurements of Carbonyl Sulfide, Hydrogen Sulfide, and Carbon Disulfide, J. Geophys. Res., 98, 23353–23372, 1993b.

Gregory, G. L., Warren, L. S., Davis, D. D., Andreae, M. O., Bandy, A. R., Ferek, R. J., Johnson, J. E., Saltzman, E. S., and Cooper, D. J.: An Intercomparison of Instrumentation for Tropospheric Measurements of Dimethyl Sulfide: Aircraft Results for Concentrations at the Parts-Per-Trillion Level, J. Geophys. Res., 98, 23373–23388, 1993c.

Hoell, J. M., Gregory, G. L., Carroll, M. A., McFarland, M., Ridley, B. A., Davis, D. D., Bradshaw, J., Rodgers, M. O., Torres, A. L., Sachse, G. W., Hill, G. F., Condon, E. P., Rasmussen, R. A., Campbell, M. C., Farmer, J. C., Sheppard, J. C., Wang, C. C., and Davis, L. I.: An Intercomparison of Carbon Monoxide, Nitric Oxide, and Hydroxyl Measurement Techniques: Overview of Results, J. Geophys. Res., 89, 11819–11825, 1984.

Hoell, J. M., Gregory, G. L., McDougal, D. S., Carroll, M. A., McFarland, M., Ridley, B. A., Davis, D. D., Bradshaw, J., Rodgers, M. O., and Torres, A. L.: An Intercomparison of Nitric Oxide Measurement Techniques, J. Geophys. Res., 90, 12843–12852, 1985a.

Hoell, J. M., Gregory, G. L., McDougal, D. S., Sachse, G. W., Hill, G. F., Condon, E. P., and Rasmussen, R. A.: An Intercomparison of Carbon Monoxide Measurement Techniques, J. Geophys. Res., 90, 12881–12890, 1985b.

Hoell, J. M., Albritton, D. L., Gregory, G. L., McNeal, R. J., Beck, S. M., Bendura, R. J., and Drewery, J. W.: Operational Overview of NASA GTE/CITE 2 Airborne Instrument Intercomparisons: Nitrogen Dioxide, Nitric Acid, and Peroxyacetyl Nitrate, J. Geophys. Res., 95, 10047–10057, 1990.

Hoell, J. M., Davis, D. D., Gregory, G. L., McNeal, R. J., Bendura, R. J., Drewery, J. W., Barrick, J. D., Kirchhoff, V. W. J. H., Motta, A. G., Navarro, R. L., Dorko, W. D., and Owen, D. W.: Operational Overview of the NASA GTE/CITE 3 Airborne Instrument Intercomparisons for Sulfur Dioxide, Hydrogen Sulfide, Carbonyl Sulfide, Dimethyl Sulfide, and Carbon Disulfide, J. Geophys. Res., 98, 23291–23304, 1993.

Singh, H. B., Brune, W. H., Crawford, J. H., Jacob, D. J., and Russell, P. B.: Overview of the summer 2004 Intercontinental Chemical Transport Experiment – North America (INTEX-A), J. Geophys. Res., 111, D24S01, doi:10.1029/2006JD007905, 2006.

Singh, H. B., Brune, W. H., Crawford, J. H., Flocke, F., and Jacob, D. J.: Chemistry and transport of pollution over the Gulf of Mexico and the Pacific: spring 2006 INTEX-B campaign overview and first results, Atmos. Chem. Phys., 9, 2301–2318, doi:10.5194/acp-9-2301-2009, 2009.
Zwolak, J. W., Boggs, P. T., and Watson, L. T.: Algorithm 869: ODRPACK95: A weighted orthogonal distance regression code with bound constraints, in: ACMTrans.Math. Softw., 33(4), Article 27(2007), 12 pp., doi:10.1145/1268776.1268782, available at: http://doi.acm.org/10.1145/1268776.1268782(last access: 11 May 2010), August 2007.

AMTD
3, 2275–2316, 2010

Measurement comparisons from INTEX-B/MILAGRO

M. M. Kleb et al.

Table 1. Chemical conditions for intercomparison periods.

Date	Air quality conditions	CO range (ppbv)
19 Mar 2006	Polluted urban and clean MBL off coast of Mexico	103–223
17 Apr 2006	Polluted and clean FT	99–163
15 May 2006	Clean FT and MBL off CA and OR coast	68–168

AMTD
3, 2275–2316, 2010

Table 2. Summary of intercomparison measurements.

Species	Technique[a]	Aircraft	Principle investigator	Uncertainty
CO	UVF	C-130	T. Campos, NCAR	10%
	DACOM	DC-8	G. Sachse, NASA LaRC	2% or 2 ppb
H_2O	Cryo	DC-8	J. Barrick, NASA LaRC, UND/NSERC	5%
	Cryo	C-130	A. Schanot, NCAR/RAF	±0.5 °C; ±1 °C below a dp of –60 °C
	DLH	DC-8	G. Diskin, NASA LaRC	5%
NO	CLD	C-130	A. Weinheimer, NCAR	10 pptv or 10%
	CLD	DC-8	D. Tan, GIT	(6.83, 85.71) 25%[b]
NO_2	CLD	C-130	A. Weinheimer, NCAR	20 pptv or 15%
	TD-LIF	DC-8	R. Cohen, UC Berkeley	15 pptv + (0.05*value)[c]
O_3	CLD	DC-8	M. Avery, NASA LaRC	3 ppb or 3% dry air, 5–7% moist air
	CLD	C-130	A. Weinheimer, NCAR	0.1 ppbv or 5%
SO_2	CIMS	DC-8	G. Huey, GIT	15%
	UVF	C-130	J. Holloway, NOAA	12% + 0.5 ppbv
	CIMS	C-130	P. Wennberg, CIT	35% + 0.2 ppbv + 0.2*formic acid
HCN	CIMS	C-130	P. Wennberg, CIT	±20% + 50 pptv
	PANAK	DC-8	H. Singh, NASA ARC	See [d]
CH_3CN	TOGA	C-130	E. Apel, NCAR	20%
	PANAK	DC-8	H. Singh, NASA ARC	See [d]
	PTRMS	C-130	T. Karl, NCAR/ACD	35%
Propanal	TOGA	C-130	E. Apel, NCAR	20%
	PANAK	DC-8	H. Singh, NASA ARC	See [d]
CH_2O	DFG	C-130	P. Weibring, NCAR	(13.45, 97.67) 17.16%[b]
	TDL	DC-8	A. Fried, NCAR	(15.15,269.8) 37.3%[b]
	EFD	DC-8	B. Heikes, URI	(17.61, 81.48) 19.3%[b]
CH_3OOH	CIMS	C-130	P. Wennberg, CIT	±50% + 150 pptv
	EFD	DC-8	B. Heikes, URI	135 + (0.25*value)
H_2O_2	CIMS	C-130	P. Wennberg, CIT	±25% + 100 pptv
	EFD	DC-8	B. Heikes, URI	±15 + (0.15*value)
	ACCD	DC-8	D. O'Sullivan, USNA	±30 ppt + 0.35*value
HNO_3	CIMS	C-130	P. Wennberg, CIT	±30% + 50 *pptv*
	TD-LIF	DC-8	R. Cohen, UC Berkeley	(23.43, 97.85) 43.7%[b]
	MC	DC-8	R. Talbot, UNH	<25 pptv = 30–35%; 25–100 pptv = 20%; >100 pptv = 15%
PAN	CIGAR	C-130	F. Flocke, NCAR/ACD	12.50%
	PANAK	DC-8	H. Singh, NASA ARC	20%
Total PANs[e]	CIGAR	C-130	F. Flocke, NCAR/ACD	12.50%
	TD-LIF	DC-8	R. Cohen, UC Berkeley	20 pptv + (0.1*value)[c]

AMTD
3, 2275–2316, 2010

Table 2. Continued.

Species	Technique[a]	Aircraft	Principle investigator	Uncertainty
NO_y-NO	CLD	C-130	A. Weinheimer, NCAR	See [d]
	TD-LIF	DC-8	R. Cohen, UC Berkeley	5%
OH	CIMS	C-130	L. Mauldin, NCAR	35%
	ATHOS	DC-8	W. Brune, Penn State	±32%
HO_2	CIMS	C-130	L. Mauldin, NCAR	35%
	ATHOS	DC-8	W. Brune, Penn State	±32%
Acetaldehyde	TOGA	C-130	E. Apel, NCAR	±20%
	PANAK	DC-8	H. Singh, NASA ARC	See [d]
	PTRMS	C-130	T. Karl, NCAR/ACD	±35%
Acetone	TOGA	C-130	E. Apel, NCAR	±20%
	PANAK	DC-8	H. Singh, NASA ARC	See [d]
Ethanol	TOGA	C-130	E. Apel, NCAR	±20%
	PANAK	DC-8	H. Singh, NASA ARC	See [d]
MEK	TOGA	C-130	E. Apel, NCAR	±20%
	PANAK	DC-8	H. Singh, NASA ARC	See [d]
	PTRMS	C-130	T. Karl, NCAR/ACD	±35%
Methanol	TOGA	C-130	E. Apel, NCAR	±20%
	PANAK	DC-8	H. Singh, NASA ARC	See [d]
	PTRMS	C-130	T. Karl, NCAR/ACD	±35%
All NMHCs	WAS	DC-8/C-130	D. Blake, UCI	5%
$j(O_3)$	SAFS	DC-8/C-130	R. Shetter, ARIM/NCAR	See [d]
$j(NO_2)$	SAFS	DC-8/C-130	R. Shetter, ARIM/NCAR	See [d]
	Filt. Rad	DC-8	J. Barrick, NASA LaRC	8%
N>3 nm	CPC	DC-8	B. Anderson, LaRC/A. Clarke, U Hawaii	10%
	CPC	C-130	A. Clarke, U Hawaii	10%
N>10 nm (15 May)	CPC	DC-8	B. Anderson, LaRC/A. Clarke, U Hawaii	5%
	CPC	C-130	A. Clarke, U Hawaii	5%
N>10 nm (17 Apr)	CPC	DC-8	B. Anderson, LaRC/A. Clarke, U Hawaii	5%
	CPC	C-130	A. Clarke, U Hawaii	5%
Hot CN (19 Mar)	CPC	DC-8	B. Anderson, LaRC/A. Clarke, U Hawaii	5%
	CPC	C-130	A. Clarke, U Hawaii	5%
Hot CN (15 May)	CPC	DC-8	B. Anderson, LaRC/A. Clarke, U Hawaii	5%
	CPC	C-130	A. Clarke, U Hawaii	5%
N_DMA	DMA	DC-8	B. Anderson, LaRC/A. Clarke, U Hawaii	See [d]
	DMA	C-130	A. Clarke, U Hawaii	See [d]
N_OPC	OPC	DC-8	B. Anderson, LaRC/A. Clarke, U Hawaii	See [d]
	OPC	C-130	A. Clarke, U Hawaii	See [d]

AMTD
3, 2275–2316, 2010

Table 2. Continued.

Species	Technique[a]	Aircraft	Principle investigator	Uncertainty
N_APS	APS	DC-8	B. Anderson, LaRC/A. Clarke, U Hawaii	See [d]
	APS	C-130	A. Clarke, U Hawaii	See [d]
Nsub	OPC	DC-8	B. Anderson, LaRC/A. Clarke, U Hawaii	See [d]
	OPC	C-130	A. Clarke, U Hawaii	See [d]
Nsuper	OPC	DC-8	B. Anderson, LaRC/A. Clarke, U Hawaii	See [d]
	OPC	C-130	A. Clarke, U Hawaii	See [d]
N_150C_DMA	DMA	DC-8	B. Anderson, LaRC/A. Clarke, U Hawaii	See [d]
	DMA	C-130	A. Clarke, U Hawaii	See [d]
N_150C_OPC	OPC	DC-8	B. Anderson, LaRC/A. Clarke, U Hawaii	See [d]
	OPC	C-130	A. Clarke, U Hawaii	See [d]
Nsub_150C	OPC	DC-8	B. Anderson, LaRC/A. Clarke, U Hawaii	See [d]
	OPC	C-130	A. Clarke, U Hawaii	See [d]
Nsuper_150C	OPC	DC-8	B. Anderson, LaRC/A. Clarke, U Hawaii	See [d]
	OPC	C-130	A. Clarke, U Hawaii	See [d]
N_300C_DMA	DMA	DC-8	B. Anderson, LaRC/A. Clarke, U Hawaii	See [d]
	DMA	C-130	A. Clarke, U Hawaii	See [d]
N_300C_OPC	OPC	DC-8	B. Anderson, LaRC/A. Clarke, U Hawaii	See [d]
	OPC	C-130	A. Clarke, U Hawaii	See [d]
Nsub_300C	OPC	DC-8	B. Anderson, LaRC/A. Clarke, U Hawaii	See [d]
	OPC	C-130	A. Clarke, U Hawaii	See [d]
Nsuper_300C	OPC	DC-8	B. Anderson, LaRC/A. Clarke, U Hawaii	See [d]
	OPC	C-130	A. Clarke, U Hawaii	See [d]
N_400C_OPC	OPC	DC-8	B. Anderson, LaRC/A. Clarke, U Hawaii	See [d]
	OPC	C-130	A. Clarke, U Hawaii	See [d]
Nsub_400C	OPC	DC-8	B. Anderson, LaRC/A. Clarke, U Hawaii	See [d]
	OPC	C-130	A. Clarke, U Hawaii	See [d]
Nsuper_400C	OPC	DC-8	B. Anderson, LaRC/A. Clarke, U Hawaii	See [d]
	OPC	C-130	A. Clarke, U Hawaii	See [d]
V_DMA	DMA	DC-8	B. Anderson, LaRC/A. Clarke, U Hawaii	See [d]
	DMA	C-130	A. Clarke, U Hawaii	See [d]
V_OPC	OPC	DC-8	B. Anderson, LaRC/A. Clarke, U Hawaii	See [d]
	OPC	C-130	A. Clarke, U Hawaii	See [d]
V_APS	APS	DC-8	B. Anderson, LaRC/A. Clarke, U Hawaii	See [d]
	APS	C-130	A. Clarke, U Hawaii	See [d]

AMTD
3, 2275–2316, 2010

Table 2. Continued.

Species	Technique[a]	Aircraft	Principle investigator	Uncertainty
Vsub	OPC	DC-8	B. Anderson, LaRC/A. Clarke, U Hawaii	See [d]
	OPC	C-130	A. Clarke, U Hawaii	See [d]
Vsuper	OPC	DC-8	B. Anderson, LaRC/A. Clarke, U Hawaii	See [d]
	OPC	C-130	A. Clarke, U Hawaii	See [d]
V_150C_DMA	DMA	DC-8	B. Anderson, LaRC/A. Clarke, U Hawaii	See [d]
	DMA	C-130	A. Clarke, U Hawaii	See [d]
V_150C_OPC	OPC	DC-8	B. Anderson, LaRC/A. Clarke, U Hawaii	See [d]
	OPC	C-130	A. Clarke, U Hawaii	See [d]
Vsub_150C	OPC	DC-8	B. Anderson, LaRC/A. Clarke, U Hawaii	See [d]
	OPC	C-130	A. Clarke, U Hawaii	See [d]
Vsuper_150C	OPC	DC-8	B. Anderson, LaRC/A. Clarke, U Hawaii	See [d]
	OPC	C-130	A. Clarke, U Hawaii	See [d]
V_300C_DMA	DMA	DC-8	B. Anderson, LaRC/A. Clarke, U Hawaii	See [d]
	DMA	C-130	A. Clarke, U Hawaii	See [d]
V_300C_OPC	OPC	DC-8	B. Anderson, LaRC/A. Clarke, U Hawaii	See [d]
	OPC	C-130	A. Clarke, U Hawaii	See [d]
Vsub_300C	OPC	DC-8	B. Anderson, LaRC/A. Clarke, U Hawaii	See [d]
	OPC	C-130	A. Clarke, U Hawaii	See [d]
Vsuper_300C	OPC	DC-8	B. Anderson, LaRC/A. Clarke, U Hawaii	See [d]
	OPC	C-130	A. Clarke, U Hawaii	See [d]
V_400C_OPC	OPC	DC-8	B. Anderson, LaRC/A. Clarke, U Hawaii	See [d]
	OPC	C-130	A. Clarke, U Hawaii	See [d]
Vsub_400C	OPC	DC-8	B. Anderson, LaRC/A. Clarke, U Hawaii	See [d]
	OPC	C-130	A. Clarke, U Hawaii	See [d]
Vsuper_400C	OPC	DC-8	B. Anderson, LaRC/A. Clarke, U Hawaii	See [d]
	OPC	C-130	A. Clarke, U Hawaii	See [d]
$SO_4^=$	MC	DC-8	J. Dibb, UNH	20%
	AMS	C-130	J. Jimenez, U CO	See [f]
	PILS	C-130	R. Weber, GIT	Conc $>2^*$LOD=20% Conc $\leq 2*$LOD=40%
NO_3^-	AMS	C-130	J. Jimenez, U CO	See [f]
	PILS	C-130	R. Weber, GIT	Conc $>2^*$LOD=20% Conc $\leq 2^*$LOD=40%

Table 2. Continued.

Species	Technique[a]	Aircraft	Principle investigator	Uncertainty
NH_4^+	AMS	C-130	J. Jimenez, U CO	See [f]
	PILS	C-130	R. Weber, GIT	Conc > 2*LOD=20% Conc ≤ 2*LOD=40%
Scatt 450nm	TSI Nephelometer	DC-8	B. Anderson, LaRC/A. Clarke, U Hawaii	See [d]
	TSI Nephelometer	C-130	A. Clarke, U Hawaii	See [d]
Scatt 550nm	TSI Nephelometer	DC-8	B. Anderson, LaRC/A. Clarke, U Hawaii	See [d]
	TSI Nephelometer	C-130	A. Clarke, U Hawaii	See [d]
Scatt 700nm	TSI Nephelometer	DC-8	B. Anderson, LaRC/A. Clarke, U Hawaii	See [d]
	TSI Nephelometer	C-130	A. Clarke, U Hawaii	See [d]
Scattsub 550nm	RR Nephelometer	DC-8	B. Anderson, LaRC/A. Clarke, U Hawaii	See [d]
	RR Nephelometer	C-130	A. Clarke, U Hawaii	See [d]
Abs 470nm	PSAP	DC-8	B. Anderson, LaRC/A. Clarke, U Hawaii	See [d]
	PSAP	C-130	A. Clarke, U Hawaii	See [d]
Abs 530nm	PSAP	DC-8	B. Anderson, LaRC/A. Clarke, U Hawaii	See [d]
	PSAP	C-130	A. Clarke, U Hawaii	See [d]
Abs 660nm	PSAP	DC-8	B. Anderson, LaRC/A. Clarke, U Hawaii	See [d]
	PSAP	C-130	A. Clarke, U Hawaii	See [d]

[a] For an explanation of "Technique", the reader is referred to the individual PI files located on the INTEX-B website (http://www-air.larc.nasa.gov/missions/intex-b/intexb.html) under the Current Archive Status link.
[b] Absolute uncertainty reported point-by-point. Percent uncertainty is calculated, minimum and maximum given in parentheses, median given outside the parentheses.
[c] Uncertainty for one second data reported point-by-point in file header. For consistency, values shown are PI estimates for 60 second averages.
[d] No PI reported uncertainty.
[e] PANs = Peroxy alkyl nitrates, formula R-C(O)OONO$_2$, with R = aliphatic, olefinic, or substituted aliphatic or olefinic substituent.
[f] Uncertainty not reported in data file header, PI refers the reader to Dunlea et al. (2009).

AMTD
3, 2275–2316, 2010

Table 3. Statistical results of DC-8/C-130 intercomparison. Note: technique is listed as X (C-130) vs. Y (DC-8).

Species	Technique	Slope	Intercept	R^2	Ratio percentiles			# Pts	Range	
					25th	50th	75th		Min	Max
a. Photochemical precursors										
CO	UVF vs. DACOM	1.09±0.00	–5.1±0.2 ppbv	0.99				7823	68.5	223
H_2O	Cryo vs. DLH	0.92±0.00	0.15±0.0 g/kg	0.99				8928	>.0006	16.5
	Cryo vs. Cryo	0.94±0.00	0.05±0.0 g/kg	0.99				9050	0.02	16.5
NO	CLD vs. CLD	0.95±0.01	13.1±0.2 pptv	0.81				5277	LOD	205
NO_2	CLD vs. TD-LIF	1.20±0.01	–39±1 pptv	0.87				2254	LOD	796
O_3	CLD vs. CLD	1.00±0.00	–1.0±0.1 ppbv	0.99				6408	26.2	133
SO_2	CIMS vs. CIMS	0.56±0.00	3±16 pptv	0.98				307	3	21610
	UVF vs. CIMS	0.86±0.01	–486±27 pptv	0.97				434	230	14700
HCN	CIMS vs. PANAK			0.37	0.50	0.69	0.90	22	150	2272
CH_3CN[a]	TOGA vs. PANAK			0.06	0.78	1.02	1.15	16	0.03	0.29
	PTRMS vs. PANAK			0.61	0.64	0.83	0.95	16	0.04	0.29
Propanal[a]	TOGA vs. PANAK			0.38	0.63	1.23	1.86	10	0.005	0.18
b. Photochemical products										
CH_2O	DFG vs. EFD	1.12±0.09	–401±152 pptv	0.88				24	LOD	3687
	DFG vs. TDL	1.01±0.03	19±33 pptv	0.95				67	LOD	3861
CH_3OOH	CIMS vs. EFD			0.30	0.87	1.13	1.41	26	217	2286
H_2O_2	CIMS vs. EFD	1.24±0.04	–19±67 pptv	0.92				74	41	2809
	CIMS vs. ACCD	0.84±0.02	313±21 pptv	0.83				392	80	2314
HNO_3	CIMS vs. MC	1.21±0.04	–3±14 pptv	0.88				98	10	1302
	CIMS vs. TDLIF			0.63	0.57	0.66	0.80	45	78	1749
PAN	CIGAR vs. PANAK	1.68±0.16	–185±59 pptv	0.77				33	2	1986
Total PAN	CIGAR vs. TDLIF	1.35±0.03	–83±10 pptv	0.94				157	LOD	2175
NO_y-NO	CLD vs. TD-LIF	0.92±0.01	51±18 pptv	0.97				143	133	5559
c. Photochemical radicals										
OH	CIMS vs. ATHOS			0.03	0.41	0.81	1.06	266	0.003	0.62
HO_2	CIMS vs. ATHOS			0.59	0.98	1.23	1.73	107	LOD	64.4
d. Oxygenated volatile organic carbons										
Acetaldehyde[a]	TOGA vs. PANAK	1.27±0.10	0.02±0.04 pptv	0.93				14	0.02	1.3
	PTRMS vs. PANAK	1.31±0.21	0.03±0.10 pptv	0.78				12	0.04	1.3
Acetone	TOGA vs. PANAK			0.50	1.05	1.42	1.82	16	0.24	3.0
Ethanol[a]	TOGA vs. PANAK							4		
MEK[a]	TOGA vs. PANAK	0.62±0.07	0.00±0.01 pptv	0.84				16	0.01	0.22
Methanol[a]	TOGA vs. PANAK			0.47	1.31	2.51	3.36	16	0.20	6.6
	PTRMS vs. PANAK			0.25	1.60	2.09	2.57	16	0.25	11.5

AMTD

3, 2275–2316, 2010

Table 3. Continued.

Species	Technique	Slope	Intercept	R^2	Ratio percentiles			# Pts	Range	
					25th	50th	75th		Min	Max
e. Nonmethane hydrocarbons										
DMS[a]	WAS vs. WAS							3	2	8
OCS[a]	WAS vs. WAS			0.41	0.98	1.00	1.01	39	451	504
CS_2[a]	WAS vs. WAS			0.30	0.96	1.58	2.53	38	3	30
CFC-11[b]	WAS vs. WAS			0.13	1.00	1.00	1.01	40	246	256
CFC-12[b]	WAS vs. WAS			0.28	1.00	1.00	1.00	40	525	538
CFC-113[b]	WAS vs. WAS			0.09	1.00	1.00	1.01	40	77	79
CFC-114[b]	WAS vs. WAS			0.06	0.99	1.00	1.01	40	15	15
H-1211[b]	WAS vs. WAS			0.25	1.01	1.02	1.03	40	4	4
H-1301[b]	WAS vs. WAS			0.00	0.96	0.99	1.00	40	3	3
H-2402[b]	WAS vs. WAS			0.19	1.00	1.00	1.02	40	0.48	0.51
HCFC-22[b]	WAS vs. WAS	0.86±0.05	23±8 pptv	0.80				40	162	180
HCFC-141b[b]	WAS vs. WAS	0.88±0.04	2.35±0.77 pptv	0.84				40	17	20
HCFC-142b[b]	WAS vs. WAS			0.51	0.98	1.00	1.02	40	15	17
HFC-134a[b]	WAS vs. WAS	0.99±0.06	0.81±2.20 pptv	0.75				40	33	41
$CHCl_3$[b]	WAS vs. WAS	1.00±0.03	0.4±0.3 pptv	0.93				40	15	17
CH_2Cl_2[b]	WAS vs. WAS	0.98±0.54	0.96±0.02 pptv	0.97				40	20	42
CCl_4[b]	WAS vs. WAS			0.13	1.00	1.01	1.01	40	91	95
C_2Cl_4[b]	WAS vs. WAS	0.99±0.03	0.05±0.12 pptv	0.94				40	1	7
C_2HCl_3[b]	WAS vs. WAS			0.48	1.72	3.89	5.59	40	0.02	1
CH_3Cl[b]	WAS vs. WAS	0.96±0.02	21±10 pptv	0.98				40	508	873
Ethylchloride[b]	WAS vs. WAS			0.63	0.84	0.96	1.05	40	2	6
CH_3Br[b]	WAS vs. WAS	0.74±0.05	2.4±0.4 pptv	0.75				40	7	10
CH_3I[b]	WAS vs. WAS	1.11±0.04	0.02±0.02 pptv	0.91				40	0.03	1
CH_2Br_2[b]	WAS vs. WAS	0.91±0.04	0.12±0.04 pptv	0.88				40	0.73	2
$CHBrCl_2$[b]	WAS vs. WAS	0.90±0.04	0.02±0.01 pptv	0.89				40	0.12	0.28
$CHBr_2Cl$[b]	WAS vs. WAS	0.91±0.04	0.02±0.01 pptv	0.85				40	0.07	0.35
$CHBr_3$[b]	WAS vs. WAS	0.92±0.03	0.07±0.03 pptv	0.92				40	0.21	3
1_2-Dichloroethane[b]	WAS vs. WAS	0.96±0.03	0.16±0.31 pptv	0.92				40	5	16
$MeONO_2$[c]	WAS vs. WAS	1.00±0.00	–0.02±0.11 pptv	0.94				40	2	5

AMTD
3, 2275–2316, 2010

Table 3. Continued.

Species	Technique	Slope	Intercept	R^2	Ratio percentiles			# Pts	Range	
					25th	50th	75th		Min	Max
$EtONO_2$[c]	WAS vs. WAS	0.93±0.03	0.10±0.05 pptv	0.95				40	0.73	3
i-$PrONO_2$[c]	WAS vs. WAS	0.96±0.04	0.06±0.20 pptv	0.88				40	0.58	9
n-$PrONO_2$[c]	WAS vs. WAS	0.94±0.04	0.02±0.03 pptv	0.86				40	0.07	1
2-$BuONO_2$[c]	WAS vs. WAS	0.86±0.03	0.01±0.18 pptv	0.85				40	0.21	11
2-$PenONO_2$[c]	WAS vs. WAS	1.29±0.08	−0.38±0.12 pptv	0.86				24	0.08	3
3-$PenONO_2$[c]	WAS vs. WAS	0.93±0.07	−0.03±0.07 pptv	0.77				25	0.06	2
3-Methyl-2-$BuONO_2$[c]	WAS vs. WAS	1.22±0.06	−0.31±0.09 pptv	0.89				24	0.04	3
Ethane[a]	WAS vs. WAS	1.00±0.01	−1.2±7.9 pptv	0.99				40	386	1664
Ethene[a]	WAS vs. WAS	1.00±0.04	−1.0±5.6 pptv	0.96				13	12	299
Ethyne[a]	WAS vs. WAS	1.00±0.01	0.06±2.7 pptv	0.99				40	32	570
Propane[a]	WAS vs. WAS	0.85±0.07	−107± 32 pptv	0.75				40	10	792
Propene[a]	WAS vs. WAS							5	4	12
i-Butane[a]	WAS vs. WAS	0.95±0.03	1.8±1.4 pptv	0.96				24	11	154
n-Butane[a]	WAS vs. WAS	0.94±0.02	3.8±1.9 pptv	0.97				24	22	416
1-Butene[a]	WAS vs. WAS							0		
Trans-2-Butene[a]	WAS vs. WAS							0		
Cis-2-Butene[a]	WAS vs. WAS							0		
1_3-Butadiene[a]	WAS vs. WAS							0		
Isoprene[a]	WAS vs. WAS							1		
i-Pentane[a]	WAS vs. WAS	0.99±0.03	1.7±1.3 pptv	0.97				24	5	181
n-Pentane[a]	WAS vs. WAS	0.96±0.03	0.18±0.72 pptv	0.96				23	5	74
2-Methylpentane[a]	WAS vs. WAS							8		
3-Methylpentane[a]	WAS vs. WAS							4	4	31
n-Hexane[a]	WAS vs. WAS	1.1±0.08	−1.9±0.66 pptv	0.97				16	4	36
n-Heptane[a]	WAS vs. WAS							1		
Benzene[a]	WAS vs. WAS	0.98±0.01	−0.29±0.78 pptv	0.99				36	4	138
1_2_4-Trimethylbenzene[a]	WAS vs. WAS							0		
1_3_5-Trimethylbenzene[a]	WAS vs. WAS							0		
Ethylbenzene[a]	WAS vs. WAS							3	4	17
i-Propylbenzene[a]	WAS vs. WAS							0		
n-Propylbenzene[a]	WAS vs. WAS							0		

Table 3. Continued.

Species	Technique	Slope	Intercept	R^2	Ratio percentiles			# Pts	Range	
					25th	50th	75th		Min	Max
f. j-values										
$j(O_3)$	SAFS vs. SAFS	1.01±0.01	0.00±0.00 s^{-1}	0.98				850	2E-5	6E-5
$j(NO_2)$	SAFS vs. SAFS	0.93±0.01	0.00±0.00 s^{-1}	0.98				867	0.009	0.015
g. Particle number and size distribution										
Toluene[a]	WAS vs. WAS	0.93±0.03	0.16±1.1 pptv	0.98				21	4	151
3-Ethyltoluene[a]	WAS vs. WAS							0		
4-Ethyltoluene[a]	WAS vs. WAS							0		
m-Xylene[a]	WAS vs. WAS							0		
p-Xylene[a]	WAS vs. WAS							0		
o-Xylene[a]	WAS vs. WAS							1		
N>3 nm	CPC	1.19±0.00	−188±36 cm^{-3}	0.93				7908	35	99 831
N>10 nm (05/15)	CPC	0.98±0.00	0.73±2.6 cm^{-3}	0.98				2981	208	3113
N>10 nm (04/17)	CPC	2.18±0.01	−191±7 cm^{-3}	0.94				2623	119	4161
Hot CN (03/19)	CPC	0.47±0.0	871±17 cm^{-3}	0.96				2290	1166	24 823
Hot CN (05/15)	CPC	0.94±0.00	−19±2 cm^{-3}	0.98				3003	70	2842
N_DMA	DMA							11		
N_OPC	OPC	0.85±0.01	0±0 cm^{-3}	0.98				149	4	886
N_APS	APS	1.81±0.01	−0.14±0.02 cm^{-3}	0.97				521	0.14	8
Nsub	OPC	0.85±0.01	0±0 cm^{-3}	0.98				149	4	884
Nsuper	OPC	1.29±0.03	−0.05±0.02 cm^{-3}	0.93				149	0.04	2
N_150C_DMA	DMA							1		
N_150C_OPC	OPC							10		
Nsub_150C	OPC							10		
Nsuper_150C	OPC							10		
N_300C_DMA	DMA							1		
N_300C_OPC	OPC							5		
Nsub_300C	OPC							5		
Nsuper_300C	OPC							5		
N_400C_OPC	OPC							10		
Nsub_400C	OPC							10		
Nsuper_400C	OPC							10		
V_DMA	DMA							11		
V_OPC	OPC	0.99±0.01	0.00±0.05 μm^3 cm^{-3}	0.98				149	0.06	9
V_APS	APS	2.62±0.05	−1.4±0.25 μm^3 cm^{-3}	0.83				521	0.13	24
Vsub	OPC	0.92±0.04	0.0±0.0 μm^3 cm^{-3}	0.98				149	0.03	6

AMTD
3, 2275–2316, 2010

Measurement comparisons from INTEX-B/MILAGRO

M. M. Kleb et al.

Table 3. Continued.

Species	Technique	Slope	Intercept	R^2	Ratio percentiles 25th	50th	75th	# Pts	Range Min	Max
Vsuper	OPC	1.14±0.03	0.0±0.0 $\mu m^3 cm^{-3}$	0.81				149	0.02	3
V_150C_DMA	DMA							1		
V_150C_OPC	OPC							10		
Vsub_150C	OPC							10		
Vsuper_150C	OPC							10		
V_300C_DMA	DMA							1		
V_300C_OPC	OPC							5		
Vsub_300C	OPC							5		
Vsuper_300C	OPC							5		
V_400C_OPC	OPC							10		
Vsub_400C	OPC							10		
Vsuper_400C	OPC							10		
h. Particle chemical composition										
$SO_4^{=}$[d]	MC vs. AMS			0.37	1.03	1.49	2.02	75	0.04	1.5
	MC vs. PILs	0.96±0.05	−0.07±0.03 $\mu g m^{-3}$	0.89				47	0.04	1.4
i. Particle scattering and absorption										
Scatt 450nm	TSI Nephelometer	1.01±0.00	−0.18±0.13 Mm^{-1}	0.99				663	2	113
Scatt 550nm	TSI Nephelometer	1.08±0.00	−0.11±0.10 Mm^{-1}	0.99				754	0.94	83
Scatt 700nm	TSI Nephelometer	1.11±0.00	−0.61±0.07 Mm^{-1}	0.99				693	1	55
Scattsub 550nm	RR Nephelometer	1.32±0.01	−0.60±0.11 Mm^{-1}	0.99				652	0.23	67
Abs 470nm	PSAP	1.09±0.02	−0.02±0.05 Mm^{-1}	0.95				112	0.04	6
Abs 530nm	PSAP	1.09±0.03	−0.04±0.04 Mm^{-1}	0.94				110	0.03	5
Abs 660nm	PSAP	1.19±0.03	−0.08±0.04 Mm^{-1}	0.91				98	0.02	4
SSA	N/A			0.27	0.99	1.00	1.01	104	0.83	0.98

[a] Online files found in VOCs link at http://www-air.larc.nasa.gov/missions/intex-b/intexb.html under the Measurement Comparisons: MILAGRO/INTEX-B/IMPEX link.
[b] Online files found in halocarbons link at http://www-air.larc.nasa.gov/missions/intex-b/intexb.html under the Measurement Comparisons: MILAGRO/INTEX-B/IMPEX link.
[c] Online files found in alkyl nitrates link at http://www-air.larc.nasa.gov/missions/intex-b/intexb.html under the Measurement Comparisons: MILAGRO/INTEX-B/IMPEX link.
[d] Further intercomparisons of the AMS with other instruments during INTEX-B have been presented by DeCarlo et al. (2008) and Dunlea et al. (2009).

AMTD
3, 2275–2316, 2010

Table 4. DC-8 intra-platform comparison.

Species	Technique	Slope	Intercept	R^2	Ratio percentiles			# Pts	Range	
					25th	50th	75th		Min	Max
a. Photochemical precursors										
H_2O	DLH vs. Cryo	1.04±0.00	–0.07±0.00 g/kg	0.99				8133	0.003	17
b. Photochemical products										
CH_2O	TDL vs. EFD	0.83±0.01	–12±8 pptv	0.88				2119	LOD	18 830
H_2O_2	ACCD vs. EFD			0.67	0.56	0.80	1.07	1962	27	9899
HNO_3	TDLIF vs. MC	0.91±0.01	–28±4 pptv	0.84				2270	3	7530
c. j-values										
$j(NO_2)$	SAFS vs. Filt. Rad.	0.96±0.00	0.00±0.00 s^{-1}	0.99				6846	LOD	0.02

Discussion Paper | Discussion Paper | Discussion Paper | Discussion Paper

AMTD

3, 2275–2316, 2010

Measurement comparisons from INTEX-B/MILAGRO

M. M. Kleb et al.

Table 5. C-130 intra-platform comparison.

Species	Technique	Slope	Intercept	R^2	Ratio percentiles			# Pts	Range	
					25th	50th	75th		Min	Max
a. Photochemical precursors										
SO_2	CIMS vs. UVF[a]	0.76±0.00	0.24±0.03 ppbv	0.90				5799	LOD	392
SO_2	CIMS vs. UVF[b]	0.87±0.00	0.07±0.02 ppbv	0.91				5854	LOD	100
CH_3CN	PTRMS vs. TOGA			0.40	0.71	0.96	1.33	1575	LOD	5.13
b. Photochemical products										
Acetic acid	CIMS vs. PTRMS			0.55	0.40	0.76	1.36	3909	LOD	10
c. Oxygenated volatile organic carbons										
Acetaldehyde	PTRMS vs. TOGA			0.50	0.68	1.24	2.58	1511	LOD	11.3
Methanol	PTRMS vs. TOGA			0.72	0.56	0.83	1.24	3442	0.02	37
d. Nonmethane hydrocarbons										
DMS	TOGA vs. WAS							44		
$CHCl_3$[c]	TOGA vs. WAS	1.25±0.03	0.20±0.22 pptv	0.86				388	5	14
$CHCl_3$[d]	TOGA vs. WAS			0.47	0.74	0.79	0.85	256	5	17
CH_3Cl	TOGA vs. WAS			0.02	0.96	1.05	1.11	287	281	1509
i-Butane	TOGA vs. WAS	1.06±0.01	0.62±3.35 pptv	0.93				455	2	608
n-Butane	TOGA vs. WAS	0.85±0.01	22.3±7.3 pptv	0.94				571	4	1634
i-Pentane	TOGA vs. WAS	1.19±0.01	13.3±3.1 pptv	0.95				523	1	938
n-Pentane	TOGA vs. WAS	0.87±0.01	4±2	0.93				471	2	436
Isoprene	TOGA vs. WAS							1		
Benzene	TOGA vs. WAS	1.26±0.02	−16.4±1.7 pptv	0.91				664	8	336
Toluene	TOGA vs. WAS	1.19±0.02	1.7±9.1 pptv	0.79				440	0.44	1112
o-Xylene	TOGA vs. WAS							91		
e. Particle chemical composition										
$SO_4^{=}$[e]	PILS vs. AMS			0.45	0.50	0.88	1.50	3669	0.02	15.8
NO_3^-[e]	PILS vs. AMS	1.54±0.03	0.15±0.10 $\mu g m^{-3}$	0.88				410	0.02	25
NH_4^+[e]	PILS vs. AMS	0.78±0.01	0.02±0.02 $\mu g m^{-3}$	0.75				2496	0.1	9.4

[a] All data. [b] $SO_2 \leq 100$ ppbv. [c] Pacific phase. [d] Mexico City phase. [e] Further intercomparisons of the AMS with other instruments during INTEX-B have been presented by DeCarlo et al. (2008) and Dunlea et al. (2009).

AMTD
3, 2275–2316, 2010

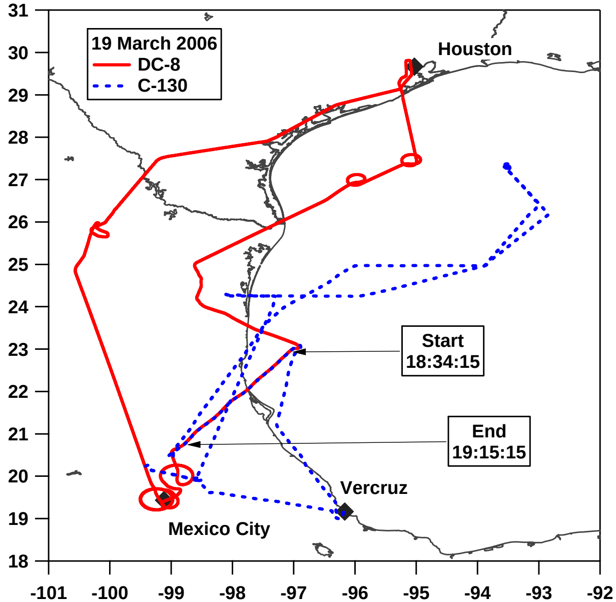

Fig. 1a. NASA DC-8 and NSF C-130 flights on 19 March 2006. The intercomparison period is indicated by the start and end times. The DC-8 flight path is shown as a solid red line. The C-130 flight path is shown as a blue dotted line.

AMTD
3, 2275–2316, 2010

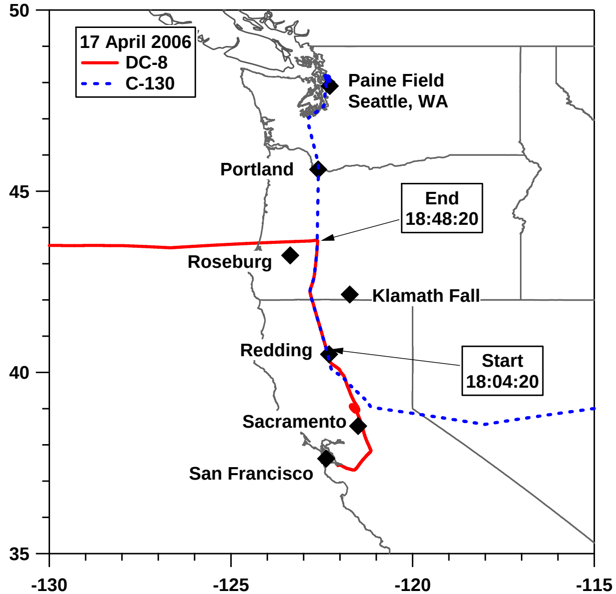

Fig. 1b. NASA DC-8 and NSF C-130 flights on 17 April 2006. The intercomparison period is indicated by the start and end times. The DC-8 flight path is shown as a solid red line. The C-130 flight path is shown as a blue dotted line.

AMTD

3, 2275–2316, 2010

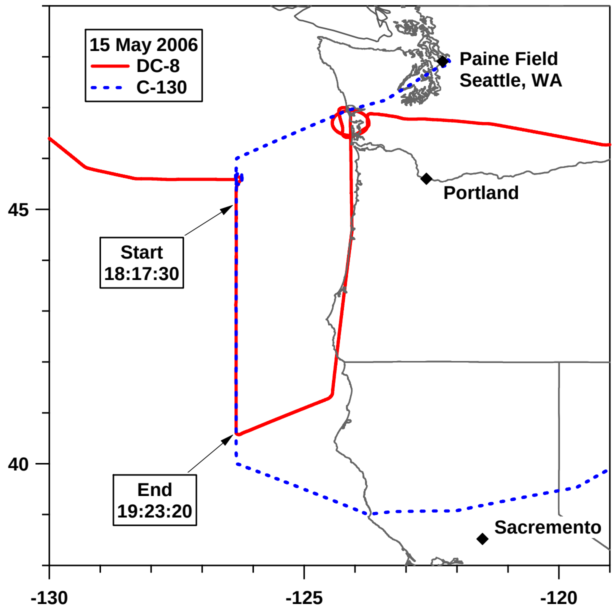

Fig. 1c. NASA DC-8 and NSF C-130 flights on 15 May 2006. The intercomparison period is indicated by the start and end times. The DC-8 flight path is shown as a solid red line. The C-130 flight path is shown as a blue dotted line.

AMTD
3, 2275–2316, 2010

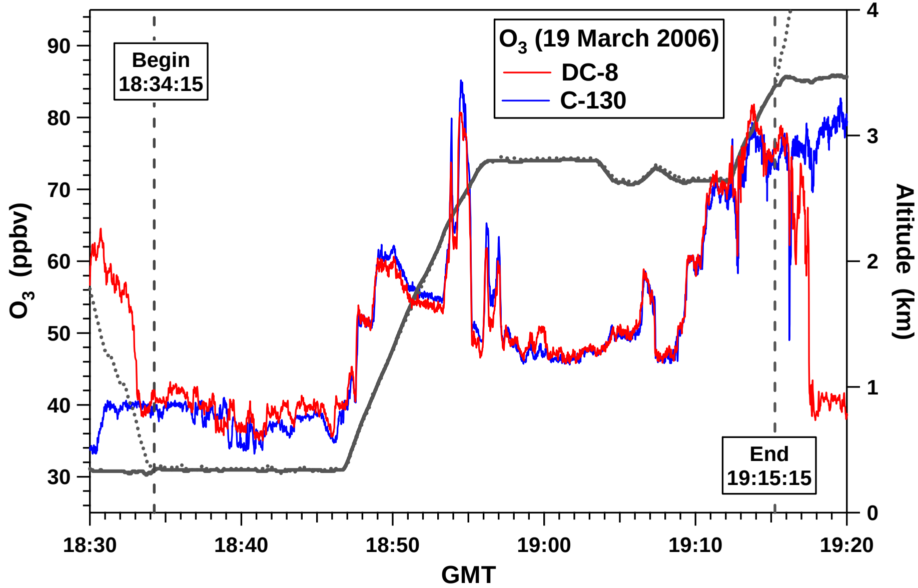

Fig. 2a. Timeseries for ozone during the intercomparison portion of the 19 March 2006 flight. The dotted gray line indicates the DC-8 altitude, solid gray line the C-130 altitude, red line DC-8 ozone, and blue line C-130 ozone.

AMTD

3, 2275–2316, 2010

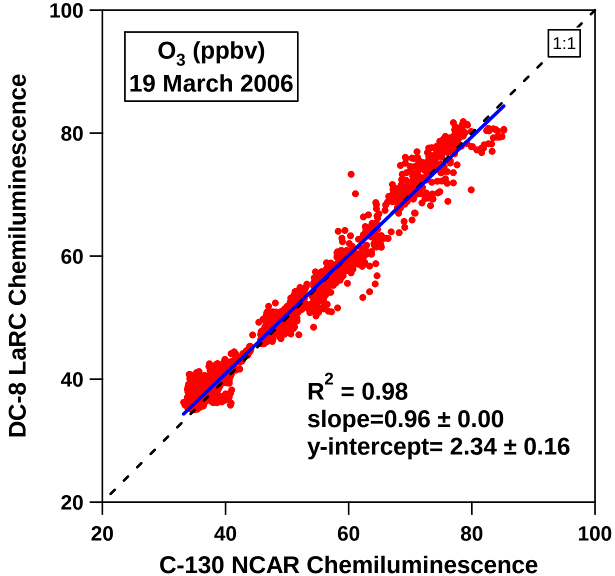

Fig. 2b. Scatter plot and orthogonal distance regression for the DC-8 and C-130 ozone intercomparison on 19 March 2006.

AMTD
3, 2275–2316, 2010

Measurement comparisons from INTEX-B/MILAGRO

M. M. Kleb et al.

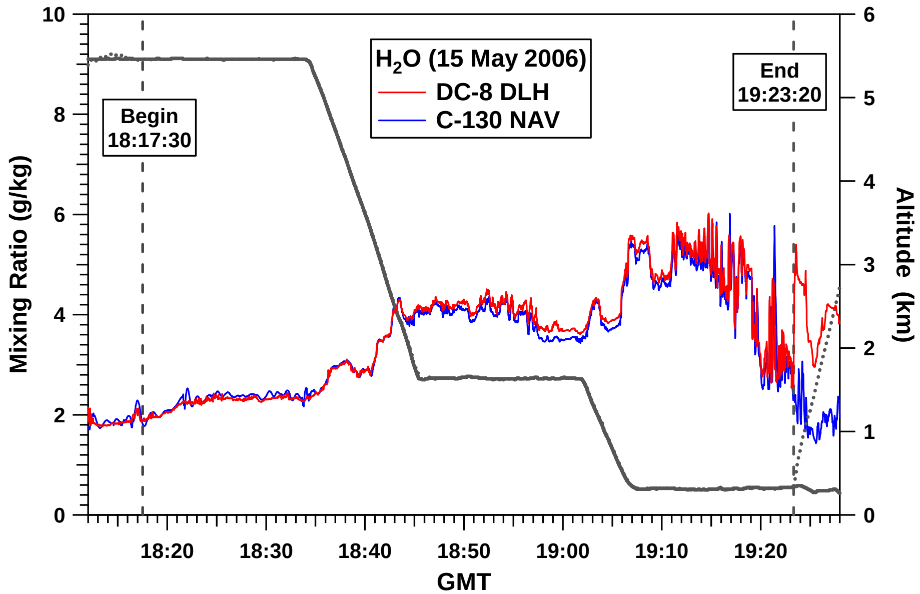

Fig. 3a. Timeseries for water during the intercomparison portion of the 15 May 2006 flight. The dotted gray line indicates the DC-8 altitude, solid gray line the C-130 altitude, red line DC-8 ozone, and blue line C-130 ozone.

AMTD
3, 2275–2316, 2010

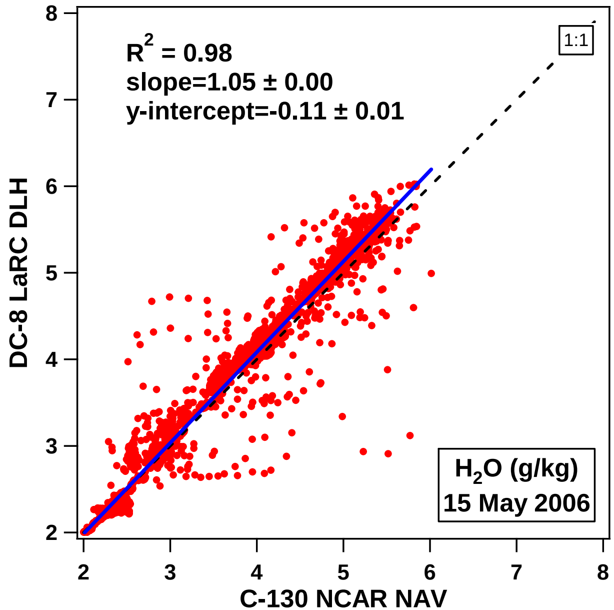

Fig. 3b. Scatter plot and orthogonal distance regression for the DC-8 and C-130 water intercomparison on 15 May 2006.

AMTD
3, 2275–2316, 2010

Measurement comparisons from INTEX-B/MILAGRO

M. M. Kleb et al.

Title Page
Abstract | Introduction
Conclusions | References
Tables | Figures
◀◀ | ▶▶
◀ | ▶
Back | Close
Full Screen / Esc
Printer-friendly Version
Interactive Discussion

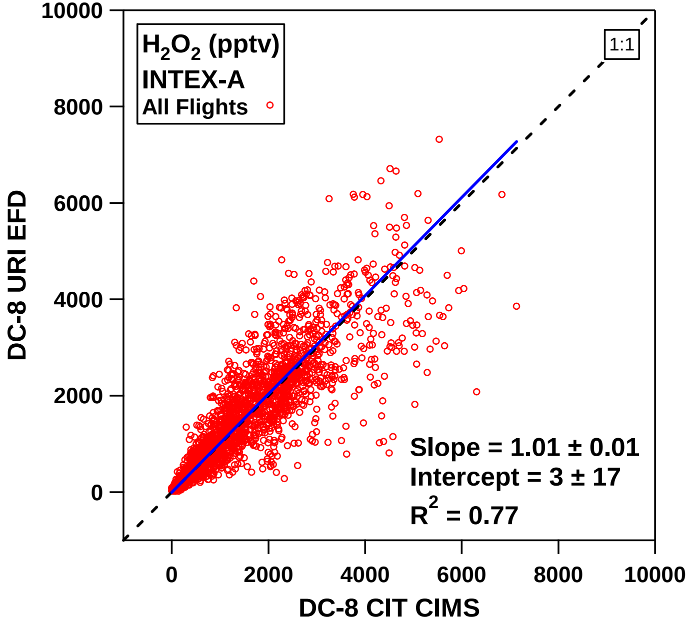

Fig. 4a. Scatter plot and orthogonal distance regression for the DC-8 CIMS and EFD H_2O_2 intercomparison of all INTEX-A flights.

AMTD
3, 2275–2316, 2010

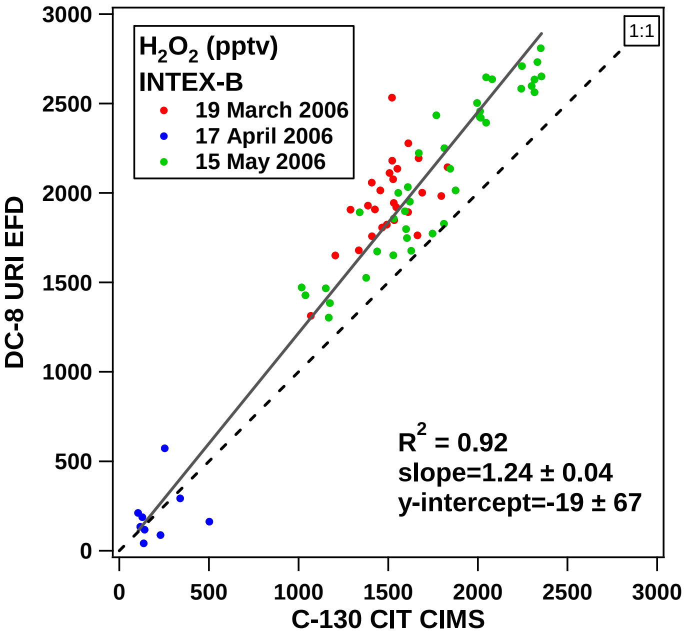

Fig. 4b. Scatter plot and orthogonal distance regression for the DC-8 and C-130 H_2O_2 INTEX-B intercomparisons on 19 March (red), 17 April (blue), and 15 May (green) 2006.

AMTD
3, 2275–2316, 2010